REPORT FOR NASA-CERES GRANT (JAN 1, 1991 - MAR 31, 2000)

This report presents highlights of the research funded under the NASA-CERES Grant titled "**A Study of Cloud Radiative Forcing and Feedback**" between Jan 1, 1991 and March 31, 2000.

The main objective of the grant proposal was to participate in the CERES (Cloud and Earth's Radiant Energy System) Satellite experiment and perform interdisciplinary investigation of NASA's Earth Observing System (EOS). During the grant period, massive amounts of scientific data from diverse platforms have been accessed, processed and archived for continuing use; several software packages have been developed for integration of different data streams for performing scientific evaluation; extensive validation studies planned have been completed culminating in the development of important algorithms that are being used presently in the operational production of data from the CERES. Contributions to the inter-disciplinary science investigations have been significantly more than originally envisioned. The results of these studies have appeared in several refereed journals and conference proceedings. They are listed at the end of this report.

The research conducted can be grouped broadly into following areas:

- CERES Window Channel:
  Concept, Design and Development

- Analysis of Water Vapor Greenhouse Effect
  Interaction between surface temperature, atmospheric greenhouse effect, water vapor and large-scale dynamics; water vapor feedback on tropical and global scales

- Formulation, Development and Testing of Different Algorithms
  Development of algorithms from physical principles

- Analysis of Storm Track Regions
  Study of summertime cloud radiative forcing in the north Pacific from ERBE data.

• Validation Studies from Different Field Experiments

CERES Window Channel: ***Design, Development and Operational Use***

A broadband window channel was proposed (CERES Science team meeting, 1989) based on its merits over the ERBE-type broadband longwave channel. Results from several sensitivity studies revealed that a window channel offers significant advantages.

Design

The CERES window filter has been designed and fabricated by the TRW Space & Technology group. We had several interactions with them and co-ordinated in achieving an optimal design for the window filter for the CERES instrument. The filter spectral response function achieved through a combination of a front and rear filter design is shown in Fig. 1.

Advantages

Among the major benefits conceived were a significant improvement in the empirical estimates of the surface net flux (LW), ability to observationally determine the water vapor greenhouse effect and monitor the non-linear rise or enhancement of the atmospheric greenhouse effect (Raval & Ramanathan, 1989) at higher surface temperatures (see Fig. 1) and provide a data base for verifying the continuum absorption in the window (8 - 12 microns). Further extensive sensitivity studies have been conducted during the following years (1991 - 1995) employing data from ERBE & NIMBUS-7, ship sondes, precipitable water from NVAP and model simulations. The results have revealed the critical importance of the CERES window channel in the following areas:

• Empirical estimates of the surface longwave flux under both clear and all-sky conditions (Inamdar & Ramanathan, 1997) ;

• Latitudinal gradients in the net longwave radiative cooling of the atmospheric column and net LW surface heating (Figs. 2-3) ;

• Water vapor greenhouse effect and its enhancement at higher surface temperatures;

• Cloud radiative forcing at the top and surface in window and broadband.

• Assessment of water vapor fedback on tropical and global scales.

These are discussed later in the report. Most of these results have also been described in a series of Journal papers and conference presentations (see appendix).

Analysis of Water Vapor Greenhouse Effect

Atmospheric greenhouse effect has been defined here as the difference in longwave emission between the surface and the top of the atmosphere (TOA) (Raval and Ramanathan, 1989 -- hereafter referred as simply RR). Since water vapor is the main absorbing constituent and is responsible for most of the observed spatial and temporal variability in the greenhouse effect, it has also been referred to as the "water vapor greenhouse effect". RR first proposed the observational determination of the greenhouse effect using the Earth Radiation Budget Data Experiment (ERBE) data. We have conducted over the past several years extensive and in-depth analysis of the atmospheric greenhouse effect integrating data from satellites, ships and GCM analysis, etc.

Some of the prominent highlights of this research are described briefly below:

(1) Surface Temperature - Greenhouse Effect Relationships

A close correlation exists between the surface temperature and the atmospheric greenhouse effect. Investigations (RR, Hallberg & Inamdar, 1993) employing satellite data to quantify the temperature dependence of the water vapor greenhouse effect (G_a) revealed that Ga increases almost linearly with SST; it was shown to be maximum over the warmest oceans such as the tropical western pacific warm pool. However, changes in surface temperature entail attendant changes in tropospheric temperature lapse rate and also humidity which influence this relationship as described below.

(2) Water Vapor - Radiative Interactions

Changes in surface temperature and humidity influence Ga and both have been found to have an equal effect in the enhancement of Ga (Inamdar and Ramanathan, 1994).

Thermodynamics (Claussiun-Clapeyron equation) dictates that a warmer atmosphere can hold more water vapor, thus suggesting the existence of a positive feedback among surface temperature, atmospheric greenhouse effect and water vapor concentration. This positive feedback was first recognized as far back as 1896 by Arrhenius. One of our recent studies (Ramanathan & Vogelmann, 1997) revisited the Arrhenius model and uncovered that water vapor feedback amplifies the surface warming by a factor of 1.3 in the model. This feedback has also been much debated in several later studies (Manabe and Wetherald, 1967; RR; Rind et al, 1991; Cess, 1991, etc). One of the main focus of our work has been to address this critical feedback issue and perform several sensitivity experiments to determine how data from the new generation of EOS satellites could be exploited to resolve this issue.

But unfortunately, although earth temperature records have been available for more than 100 years, simultaneous measurement records for the atmospheric column precipitable water vapor and/or satellite radiometric observations covering the entire globe have been lacking to either strongly support or refute positive water vapor feedback. However, we performed a detailed investigation (Inamdar & Ramanathan, 1998) employing a host of data sets from several different sources extending analysis in geography and time and encompassing both land and oceans. This work represents the first time an attempt has been to include both land and oceans in the analysis of the atmospheric greenhouse effect aimed at getting a better handle of the global water vapor feedback issue. This study appeared in a special EOS edition of the Journal of Geophysical Research among a series of select studies dealing with the science and data analysis planned for the EOS AM & PM platforms. The investigations in the study employed both GCM model simulations (IPCC, 1995) and observational studies in the form of the ERBE data record (1985 - 89) and annual to interannual cycles.

Two of the key results of the study are depicted in Figs. 4-5. Fig. 4 shows the global average atmospheric greenhouse effect separated into oceans, land & combined. Fig. 5 shows the feedback sensitivity parameter dGa/dTs derived from the annual cycle for successively larger domains extending on either side of the equator all the way to the poles. When averaged from the southern to the northen latitudes these parameters exhibit a statistically significant estimate for the feedback represented by the dGa/dTs term (Inamdar & Ramanathan, 1998). The basic inference from Fig. .. is that the Ga-sensitivity derived from several different approaches converge for the globe into a domain identified as positive feedback. Irrespective of the region (ocean or land) or the latitude domain

(tropics or extra-tropics), the data presented here do not offer any support for the suggestion that increases in tropical or global mean surface temperature would lead to a decrease in water vapor greenhouse effect by drying the middle to upper troposphere. If any, the global sensitivity derived from the annual cycle is consistent with the magnitude of the positive feedback obtained by general circulation models.

(3) Supergreenhouse effect

A recurrent phenomenon observed in the surface temperature - greenhouse effect relationships has been the enhancement of Ga in the tropics for higher values of surface temperatures. While most of the increase in Ga with increasing Ts could be attributed to the thermodynamic increase in the atmospheric water vapor content (RR, Stephens and Greenwald, 1991), RR study also uncovered a rapid rise in Ga for ocean surface temperatures exceeding about 298 K. This increase in Ga which exceeded the rate at which the surface emissions increase (about 6 W m-2 K-1) was termed the "supergreenhouse effect" (a term coined by Vonder Haar, 1986), and is found to occur at all spatial and temporal scales. This enhancement of the greenhouse effect represents an unstable clear-sky longwave radiative feedback which calls for a counter-feedback to stabilize the surface temperatures. A mere thermodynamically-induced water vapor increase nor a steepening of the lapse rate with higher surface temperature were found inadequate to explain the phenomenon. Model simulations (Hallberg & Inamdar, 1993) and extensive observation studies (Rind et al, 1991; Flohn et al, 1989) uncovered a need for a significant moistening of the mid to upper troposphere of the tropical deep convective regions to cause the enhanced greenhouse effect.

Further, studies have also uncovered that most of the enhancement in Ga manifests in the window region (Fig. ..) suggesting the key role of the continuum in the supergreenhouse effect. The excess moisture in the deep convective regions is presumably supplied through a CISK-type (Convective Instabilities of the Second Kind) mechanism (Holton, 1992 ed), whereby low-level convergence transports extra moisture into the mid and upper troposphere (Inamdar and Ramanathan, 1994).

(4) Upper troposphereic drying ?

All the afore-mentioned investigations have explored the physics of the atmospheric greenhouse effect and attempted to unravel the interactions between surface temperature,

greenhouse effect and the dynamics of water vapor transport in the earth's atmosphere. While the results have not convincingly established a positive water vapor feedback yet, they do not support a negative feedback either as proposed by some studies (Lindzen, 1990). Lindzen's study hypothesized that deep convection tends to dry the mid to upper troposphere in the tropics. Some other studies (Lindzen, 1994; Lindzen et al, 1995; Bony et al 1995; Lau et al 1996) also supported this view maintaining that the supergreenhouse effect is a domain-specific phenomenon, being strongly influenced by the circulation patterns elsewhere, and hence does not necessarily imply a positive feedback. But a suitable natural experiment proposed by Lindzen (Lindzen et al, 1995) himself has been undertaken to test the drastic difference between the two contradictory hypothesis. This involved examining the global annual cycle of variation in greenhouse effect, surface temperature and water vapor, employing a multitude of data sets (Inamdar and Ramanathan, 1998). The results based on the annual and inter-annual cycles suggest the existence of supergreenhouse effect (in the tropics) even when both the limbs of Hadley and Walker circulation are included. Although the annual cycles of tropospheric temperatures are not an exact analogue of longer time scale changes, the data do not offer any support for the global negative feedback effect consistent with the cumulus drying hypothesis of Lindzen.

A major drawback here has been again the lack of long-term satellite observations and a reliable source of atmospheric temperature and water vapor profiles in testing the hypothesis. The record of CERES observations alongwith other correlative variables should at least partially fullfil these needs.

(5) Vertical sensitivity of spectral variation of water vapor greenhouse effect

Both model (Clough et al, 1992; Sinha and Allen, 1994; Sinha and Harries, 1995) and a few observation studies (Harries, 1997; Carli and Park, 1988) have highlighted the importance of investigating the spectral variation of water vapor greenhouse effect in validation of models of climate change. For instance, the sensitivity of the OLR to the lower tropospheric water vapor is greatest in the 8 - 12 μm window region, while the sensitivity to upper tropospheric water vapor perturbations is largest in the non-window region comprising the pure rotation bands (greater than 12 μm) and vibration-rotation bands (less than 8 μm). The normalized greenhouse effect has been found to be the most sensitive in the far infrared (greater than 20 μm) for the Subarctic Winter atmosphere and

in the window (8 - 12 μm) for the tropical atmosphere (Sinha and Harries, 1995). Yet there have been very few measurements of absorption in the far infrared spectrum.

The window channel (8 - 12 μm) of the CERES instrument offers us a strategy to spectrally decompose the atmospheric greenhouse effect into different bands and examine their relationships to tropospheric water vapor distribution. Some preliminary studies have been undertaken employing rawinsonde data plugged into a radiative transfer model and matching the calculated flux with CERES footprints. The results will help in understanding the physics of water vapor absorption in the window and non-window and observations of broadband and window flux from the CERES are expected to reveal critical information pertaining to the distribution of moisture in the troposphere.

Algorithms for Estimating the Surface Longwave Flux

As members of the CERES Algorithm Development and Data Management Team, we have worked towards contributing to the CERES Experiment through formulation, design, development, testing and integration of operational algorithms for estimating the surface LW flux under cloud-free conditions over both oceans and land surfaces. The back radiation from the atmosphere to the surface, representing the radiative heating of the surface by the atmosphere constitutes an additional important measure of the atmospheric greenhouse effect (Inamdar & Ramanathan, 1997). The analysis technique which has been developed derives this measure from a combination of OLR (broadband & window), surface temperature, column precipitable water and near-surface air temperature (Fig. ..). The potential benefits of the CERES window channel in the estimation of the downward LW flux, addressing water feedback and continuum-related studies has been demonstrated by us.

Link Between Summertime Cloud Radiative Forcing and Extra-tropical Cyclones in the North Pacific

This work was conducted by a graduate student, Chris Weaver, working for his doctorate.

This study (Weaver & Ramanathan) explores the interactions between cloud radiative forcing and large-scale dynamics and thermodynamics over the extra-tropical North Pacific and North Atlantic. The geographic correspondence between monthly mean fields of cloud radiative forcing, cloud type and optical depth, and quantities such as

baroclinicity and transient eddy flux suggests that large-scale, stratiform cloud systems associated with traveling cyclones are largely responsible for the band of strongly negative shortwave cloud forcing (C_S) over the Pacific between 40^0 and 60^0 N. Analysis of daily ERBE cloud forcing for July 1985, in conjunction with daily ECMWF geopotential, demonstrates the evolution of highly reflective cloud systems associated with several traveling, closed lows. The southwest to northeast extension of the broad maximum in monthly mean C_S magnitude is in agreement with the observed pattern of traveling cyclones whose genesis is near Japan and Korea and whose trajectory continues to the Aleutian Islands and the Gulf of Alaska.

Validation Studies

We have employed data from the different field experiments initiated by the Center for Clouds, Chemistry and Climate under NSF funding, to perform many validations. These are detailed below.

(1) Central Equatorial Pacific Experiment (CEPEX)

This was a multi-platform field experiment conducted during Mar/Apr 1993, involving measurements from ships, aircraft and satellites. Sonde measurements were made aboard the R/V Vickers ship which sailed along the equator. The ship also housed a pyrgeometer (Grassl group) and an FTIR (Fourier Transform Spectro Radiometer instrument placed by Dan Lubin) to measure respectively the broadband and spectral (5 - 20 microns) downwelling longwave radiation. Together with the sonde data, they provided an excellent data set to perform a semi-validation of the algorithms described earlier. These have been reported in a published paper (Inamdar & Ramanathan, 1997 Tellus), several Science team meeting reports and presentations at Conference/Symposia.

(2) Indian Ocean Experiment (INDOEX)

This was a multi-national major field experiment conducted in the Indian Ocean between 1997 - 1999. The U.S. component was funded by NSF and involved premier environmental scientists, universities and national laboratories from the U.S., Europe and Indian Ocean region. The experiment generated a wealth of data immensely useful in vaildation studies, from a diverse array of platforms including ships, satellite, aircraft and surface observatories.

During the last year, our team undertook the validation of CERES data with data collected during the First Field Phase (FFP) of the INDOEX project. The FFP was conducted during Feb 22 to March 31 of 1998. The data was collected from the following platforms:

(1) Kaashidhoo Climate Observatory (KCO) in the island of Kaashidhoo (74E, 4N), in the Maldives. The instruments used in the study were shaded and unshaded pyranometers, shaded and unshaded photo diode radiometers, operating in the 0.4 to 0.7 mm, CIMEL sun photometer (for aerosol optical depths in seven wavelengths), aerosol chemical composition measurements, aerosol single scattering albedo and absorption measurement and LIDAR.

(2) Research Vessel Sagar Kanya, cruising between 20 N and 25 S in the Indian Ocean between 65E to 75E longitude, included instruments: Vaisala water vapor sondes, the radiometers mentioned above mounted on gimbals (only unshaded), Sun photometer, Grating Spectrimeter and LIDAR.

(3) SeaWifs aerosol optical depths

(4) AVHRR Aerosol Optical Depths

The validation was conducted, employing CERES ERBE-like ES8 data sets, as follows:

- **Comparison of CERES LW Fluxes with Model Results**

  Class sonde measurements made aboard the R/V Sagar Kanya have been employed as input to the standard radiative transfer model and top-of-atmosphere (TOA) fluxes in the broadband and window regions evaluated. Broadband and window fluxes have been derived from the CERES-measured radiances using an updated ADM model (developed by Norman Loeb). The CERES scan footprints were collocated with the ship location within a 6 hour time window. The agreement between the model and measurements for clear sky conditions was found to be very good.

These comparisons have been repeated by employing the NMC Upper air data over land surface stations in *lieu* of ship sondes for the period Jan - Apr 1998.

• CERES TOA Albedos

The Cloud and Earth's Radiant Energy System (CERES) radiometer is perhaps the best broad band radiometer flown in space, with an absolute accuracy of 0.2 % or better and a comparable precision. Calibration of the instrument (instrument gain) has changed by less than 0.1% in 9 months of space flight. The CERES measures the radiance and these are then converted to irradiances (fluxes), using empirical algorithms [Wielicki et al, 1996]. As a result, the irradiances are subject to larger uncertainties (than the radiances). With respect to the present study, it should be noted that the least uncertainty in these algorithms are shown to be for clear sky oceanic regions [e.g., see Ramanathan et al, 1989], which are the only cases considered in this study.

We have compared the TOA clear sky albedo from CERES with the model results for KCO. Due to the low inclination orbit, we could get only one day time measurement over the Arabian sea; the pixel size varies from about 10 km (for nadir) to about 30 km for slant viewing angle (say 60 deg). The following criteria were used to select the CERES data: The time of CERES clear sky measurement should match the time of KCO clear sky data within 15 minutes; and the spatial location of CERES clear sky pixel should be within 25 km of KCO. The data and model albedos agree excellently (within about 0.005), when the solar and satellite angles are less than 50^0 (Satheesh et al, 1999), and for the few data points when these angles exceed 500 (slant angles), the differences exceed 0.03. We propose the following reasons for the larger difference for the slant angles: First, The algorithms for converting satellite radiances to fluxes are particularly prone to errors for slant solar and viewing angles; and second, cloud contamination of scenes is more likely for slant satellite viewing angles (note that there is a systematic difference, with CERES albedos always larger for the slant angles).

ANALYSIS TOOLS

Over the course of past several years, we have accessed, archived and processed massive amounts of data including rawinsonde data from ship and land stations, satellite data (ERBE, AVHRR, etc), GCM analysis products (GEOS, ECMWF and NCEP), NASA water vapor (NVAP), microwave precipitable water, surface emissivities for land stations, in addition to the vast amonts of data from the special field experiments (CEPEX & INDOEX) sponsored by the Center for Clouds, Chemistry and Climate. Several models and specialized software tools for the analysis of these data sets characterized by different temporal and spatial resolutions have been developed. Some of these are described below.

Data Sets Available

ERBE: The center has archived S4, S8 and S9 categories of data and an array of software tools to process, analyze and visualization of ERBE in conjunction with other correlative data. This is the most extensively used data set.

Surface Temperatures: We have developed and archived data from different sources for the surface temperatures covering the entire globe. Over the oceans, we have used the NMC-blended analysis (Reynold's, 1988). This covers the period since 1982. Prior to 1982, due to lack of any available satellite data, we make of use of the Global Ice and Sea Surface Temperature (GISST) data compiled by David Parker and his team at the UK Metereological office.

For land surface temperatures, we use a variety of sources. One of them is the Goddard Assimilated data products (Schubert et al, 1995). These assimilations are undergoing revision and are expected to be of improved quality in the future. We have also developed a monthly gridded means of surface temperatures over land using the NMC archives of daily station surface temperatures. Presently this covers the period 1979 - 1988 over a 1 by 1 degree grid. This will be extended to include other years. Further the group led by P.D. Jones at the Climate Research Unit of the University of East Anglia is developing a 0.5^0 latitude by 0.5^0 longitude surface climatology of global land areas and the monthly

anomalies. Arrangements have been made to access this data as soon as it becomes available.

NVAP (Nasa Water Vapor Project): This is the source of our precipitable water vapor data representing a blended analysis of microwave, TOVS and rawinsonde network covering the globe (Randel et al, 1995). It includes three levels of column-integrated water vapor in the troposphere. It is available since 1988 and has already been used in our earlier study (Inamdar & Ramanathan, 1998).

Land Surface Properties: Since land surfaces do not emit as black bodies and also the surface albedos are variable depending upon the nature of the surface, we have employed the surface emissivity data compiled by Dave Kratz et al (1999) based on the vegetation indices of Salisbury et al. In future, we plan to make use of the measurements from the high spatial resolution instrument ASTER, to be flown alongwith CERES, MODIS and MISR on board the EOS AM platform.

Gridded Land Surface Temperatures. We have compiled NMC station surface data for the years 1979 - 1989 for daily surface temperatures and have processed these data sets into a 1 by 1 degree and also a 2.5 by 2.5 degree latitude - longitude grids and monthly averages for compatibility of processing alongwith ERBE and other related data sets. The time series will be extended in future to cover other years.

The C4 CIDS (described below) data base also includes among others the NIMBUS 7 scanner and non-scanner data in a netcdf format, a 10-year data base of ship sondes, Hahn's synoptic cloud reports between 1982 - 1991 including low, mid and high level clouds with a unique overlap processing scheme developed by us. The CIDS data tool can also collocate these data sets in time and space with other satellite, ship or aircraft data according to user-specified criteria.

Analysis Tools

Modified version of LOWTRAN 7/MODTRAN Code: We have a modified version of the AFGL-developed Low Resolution Transmittance code (Kneizys et al, 1988) to perform accurate longwave radiative transfer calculations in the earth's atmosphere. The modifications (described in Inamdar and Ramanathan, 1997) include a high resolution vertical quadrature scheme, use of the latest and revised water vapor continuum

absorption (Clough et al, 1994) coefficients and a delta-Eddington type approach to perform LW radiative transfer through thin cirrus clouds. With some effort, this code can be easily adapted for the higher spectral resolution version MODTRAN.

The following tools, extremely useful in remote sensing applications, have been developed at C4 using NSF and DOE (ARM) funds. They have been used extensively in many validation studies also.

3-D Radiative Transfer Code: A technique (Galinsky and Ramanathan, 1998) for solving the radiative transfer in weakly horizontally inhomogeneous medium has been obtained in the diffusion approximation using the expansion of the three dimensional delta-Eddington approximation. The solution has been compared to the results of numerical simulations for the three-dimensional radiative transfer equation using the spherical harmonics discrete ordinate method yielding good agreement. This technique is planned to be used in the remote sensing of clouds from satellite imagery.

3-D Monte Carlo Code: The 3-D Monte Carlo code (Podgorny and Vogelmann, 1998) developed at C4 using the DOE funds is another useful tool in climate applications. This method has also been validated against the discrete ordinate method, has a flexible spectral resolution and can handle any cloud configuration. It is proposed to be used on satellite pixel scales to obtain heating rates in clouds.

Algorithm to process satellite cloud imagery: One of the investigators has developed a Lagrangian approach (Boer & Ramanathan, 1997) for identification and classification of clouds. The algorithm can analyze any cloud imagery (especially from Geostationary satellites) and track its evolution in space and time.

C4 Integrated Data System (CIDS): The center has developed (under NSF funding) a very sophisticated tool for the integration, analysis and visualization of meteorological and satellite data referred to as the "C4 Integrated Data Systems (CIDS)". The system can handle multi-platform data (satellites, aircraft, ships, surface stations) and perform collocations of these data in space and time. The software tool is user-friendly and has a dedicated team of programmers working.

CERES-Supported List of Publications

Standard Refereed Journals

Raval, A., and V. Ramanthan, 1989: Observational determination of the greenhouse effect. Nature, **342**, 758-761, 1989.

Ramanthan, V., and W. Collins, 1991: Thermodynamic regulation of ocean warming by cirrus clouds deduced from observations of the 1987 El Nino. Nature, **351**, 27-32, 1991.

Inamdar, A.K., and V. Ramanathan, 1992: Greenhouse effect over the tropical oceans: Relative importance of water vapor and lapse rate variations. *IRS '92: Current Problems in Atmospheric Radiation, Proceedings of the International Radiation Symposium*, Tallinn(Estonia), Aug 1992. Ed S. Keevallik and O. Karner, 155-157.

Cess, R.D., E.F. Harrison, P. Minnis, B.R. Barkstrom, V. Ramanathan et al, 1992: Interpretation of seasonal cloud-climate interactions using Earth Radiation Budget Experiment Data. *J. Geophys. Res.*, **97**, 7613-7617.

Hallberg, R., and A.K. Inamdar, 1993: Observations of seasonal variations in atmospheric greenhouse trapping and its enhancement at high sea surface temperature. *J. Climate*, **6**, 920-931.

Inamdar, A.K., and V. Ramanathan, 1994: Physics of greenhouse effect and convection in warm oceans. *J. Climate* , **7**, 716-731.

Collins, W.D., and A.K. Inamdar, 1993: Variation of clear-sky fluxes for tropical oceans from the earth radiation budget experiment. *J. Climate* , **8**, 569-578.

Ramanathan, V., B. Subasilar, G. Zhang, W. Conant, R. Cess, J. Kiehl, H. Grassl and L. Shi, 1995: Warm pool heat budget and shortwave cloud forcing: A missing physics ? *Science,* **267**: 499-503.

Weaver, C. P., and V. Ramanathan, 1995: Deductions from a simple climate model - factors governing surface temperature and atmospheric thermal structure. *J. Geophys. Res.*, **100,** 11585-11591.

Inamdar, A.K., and V. Ramanathan, 1996: On inferring global scale water vapor feedback using surface and space-based observations. In IRS'96: *Current Problems in Atmospheric Radiation*, Edited by W.L. Smith and K. Stamnes, pp 730-733., A. Deepak Publishing, 1067 pp.

Weaver, C.P., and V. Ramanathan, 1996: The link between summertime cloud radiative forcing and extratropical cyclones in the North Pacific. *J. Climate*, **9**, 2093-2109.

Weaver, C.P., and V. Ramanathan, 1996: Relationships between large-scale vertical velocity, static stability, and cloud radiative forcing over northern hemisphere extratropical oceans. *J. Climate,* **10**, 2871-2887.

Weaver, C.P., 1996: Dynamical and thermodynamical controls on large-scale cloud radiative forcing over northern hemisphere extratropical oceans. Ph.D.Thesis, University of California, San Diego.

Inamdar, A.K., and V. Ramanathan, 1997: On monitoring the planetary greenhouse effect from space, *Tellus*, **49B**, 216-230.

Ramanathan, V., and A.M. Vogelmann, 1997: Greenhouse effect, atmospheric solar absorption and the earth's radiation budget: from the Arrhenius-Langley era to the 1990s. Ambio, **26**, 38-46, 1997.

Ramanathan, V., 1998: Trace-gas greenhouse effect and global warming - Underlying principles and outstanding issues - Volvo Environmental Prize Lecture - 1997. *Ambio*, **27** N3:187-197.

Conant, W. C., A. M. Vogelmann, and V. Ramanathan, 1998: The unexplained solar absorption and atmospheric H2O: A direct test using clear-sky data. *Tellus*, **50A**, 525-533.

Inamdar, A.K., & V. Ramanathan, 1998: Tropical and global scale interactions among water vapor, atmospheric greenhouse effect, and surface temperature. *J. Geophys. Res.* (EOS Special Issue), **103**, 32,177-32,194.

S.K. Satheesh, V. Ramanathan, X.L. Jones, J.M. Lobert, I.A. Podgorny, J.M. Prospero, B.N. Holben and N.G. Loeb, 1999: A Model for Natural and Anthropogenic Aerosols over the Tropical Indian Ocean Derived from INDOEX data, *J. Geophys. Res.*, **104**, 27,421-27,440.

Symposia/Conferences

Inamdar A.K., and V. Ramanathan, 1992: More on the water vapor greenhouse effect over the tropical oceans. Presented at *AGU 1992 Spring meeting*, Montreal, May 1992.

Inamdar, A.K., and V. Ramanthan, 1992: Super greenhouse effect over the tropical oceans: relative importance of water vapor and lapse rate variations. *International Radiation Symposium,* Tallinn(Estonia) Aug 3-8 1992.

Inamdar, A.K., H.G.J. Smit and D. Kley, 1993: The relationship between greenhouse effect and deep convection based on simultaneous observations of tropospheric ozone and water vapor. Presented at *AGU 1993 Fall Meeting*, San Francisco, Dec 1993.

Inamdar, A.K., and V. Ramanathan, 1994: Retrieval of surface longwave radiation budget from satellite radiometric measurements using CERES instrument. EOS (Supplement) April 19 of AGU Spring Meeting, May 1994.

Inamdar, A.K., and V. Ramanathan, 1998: Water vapor feedback derived from annaul cycles. Presented at the AGU Fall 98 Meeting, San Francisco, CA, Dec, 1998.

Ramanathan, V., and A. K. Inamdar, 1998: Water vapor feedback in the tropics. 23rd Conference on Hurricanes and Tropical Meteorology, 79th AMS Annual Meeting, Dallas, Texas, Jan 1998.

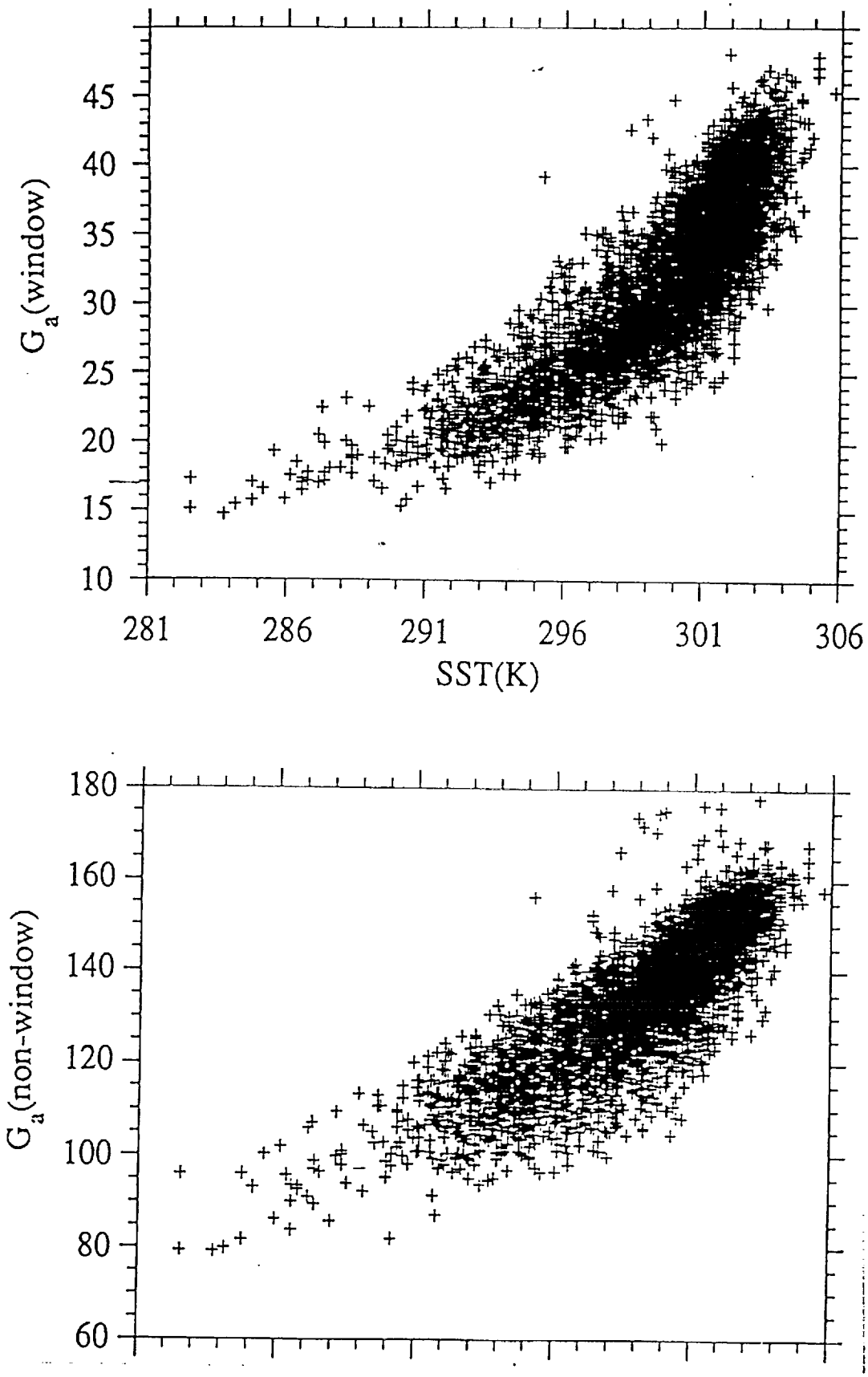

Fig. 1. Window (8 - 12 mm) and non-window components of greenhouse effect as a function of SST from model simulations using 5 year ship sondes as input (Source: Inamdar & Ramanathan, 1994).

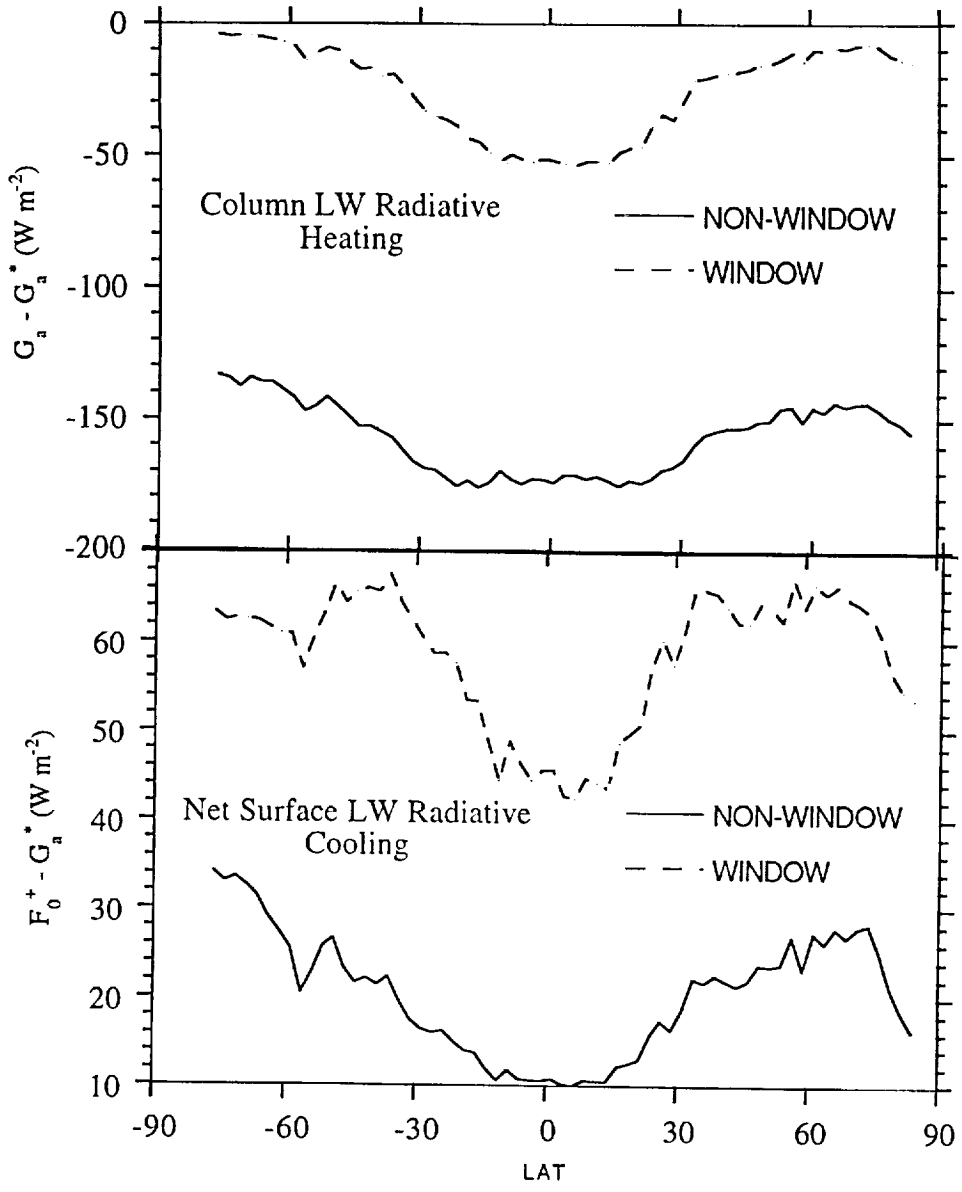

Fig. 2 Water vapor continuum plays an important role, not only in the seasonal variation, but also in the latitudinal gradient. It is just as important as the non-window region in determining the latitudinal gradient in the atmospheric LW radiative heating (top panel) and is the dominant source of the net surface LW radiative cooling in the tropics (bottom panel). For example, at the equator, the window cooling at the surface is about 40 W m^{-2}, while the non-window cooling is only 10 W m^{-2}. (Inamdar & Ramanathan, 1997)

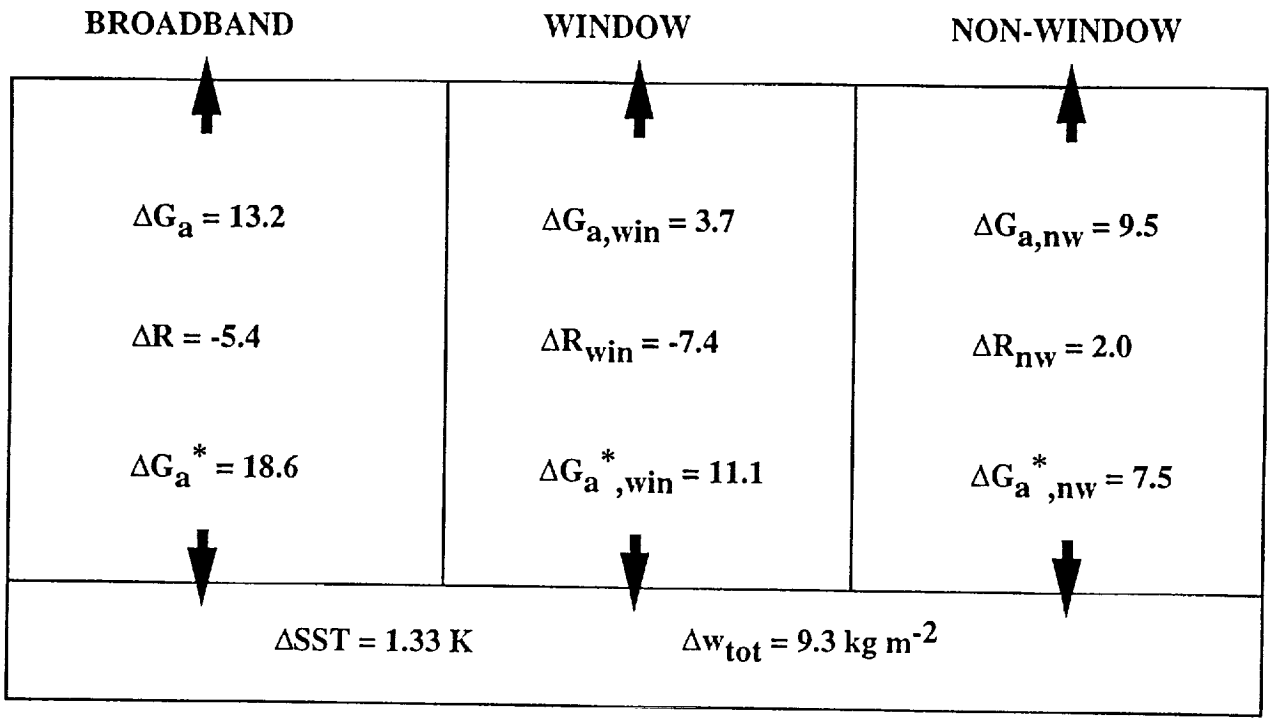

Changes in the atmospheric greenhouse effect (ΔG_a), surface flux (ΔG_a^*) and atmospheric radiative cooling ($\Delta R = \Delta G_a - \Delta G_a^*$) between JJA and DJF seasons for all oceans ($0 - 25^0$ N). The respective window and non-window components of the changes are shown in the center and right panels. SST is the ocean surface temperature and w_{tot} represents the total column precipitable water. It is evident that window accounts for a major fraction of the change in the surface flux. Interestingly, the atmospheric LW radiative cooling (represented by the ΔR terms) in the window exceeds the total, while there is a slight heating of the tropospheric column in the non-window spectral regions.

Fig. 3

GLOBAL AVERAGE ATMOSPHERIC GREENHOUSE EFFECT (W m^{-2})

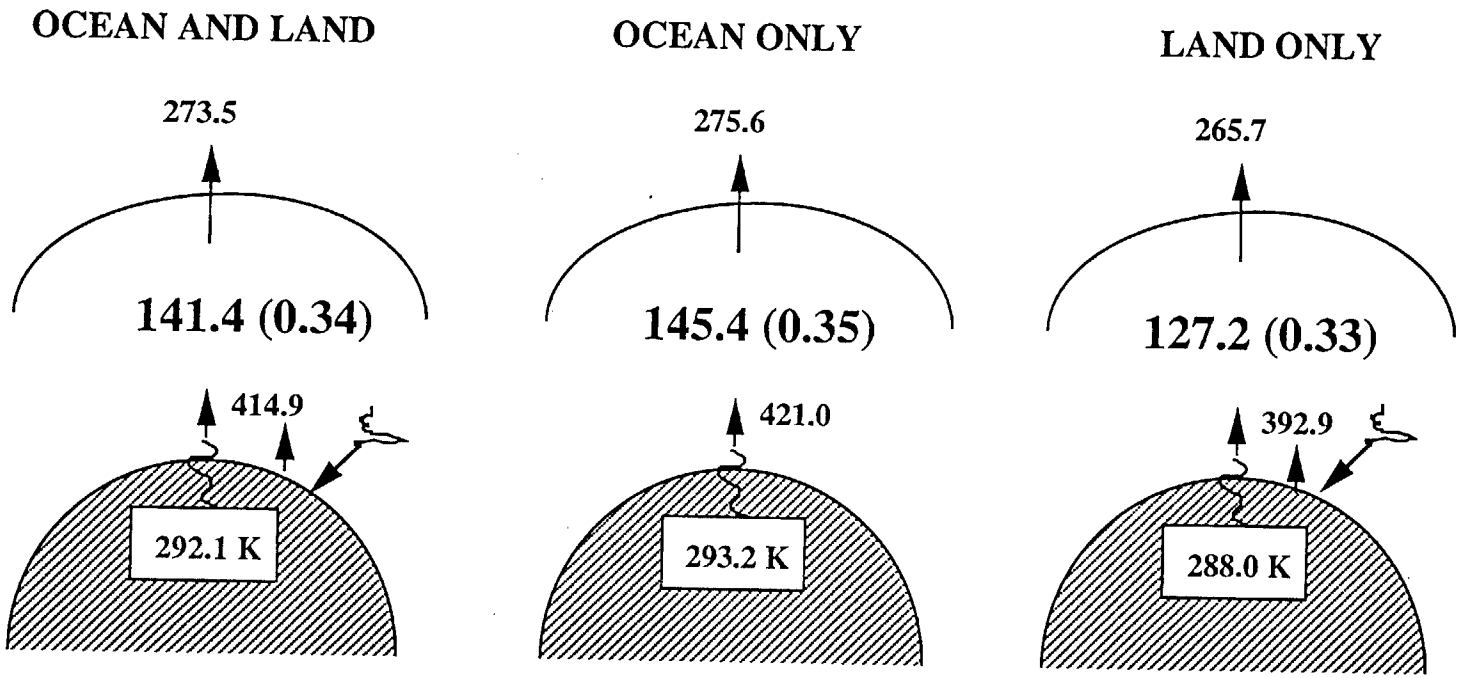

Results shown are for the ice-free earth (approximately 94 % of the Earth's surface)

Uncertainties:
surface emission: ± 3 W m^{-2}, TOA flux: ± 5 W m^{-2}, G_a: ± 5 W m^{-2}

Fig. 4

Global average of surface temperature, surface emission, outgoing longwave radiation, and atmospheric greenhouse effect derived from ERBE, NMC-blended sea surface temperature (SST) (for the oceans), NMC station surface temperatures (for the land), and surface emissivities based on Salisbury et al (1992) vegetation index tables, for the period 1988-89. Results exclude ice-covered regions. (Inamdar & Ramanathan, 1998)

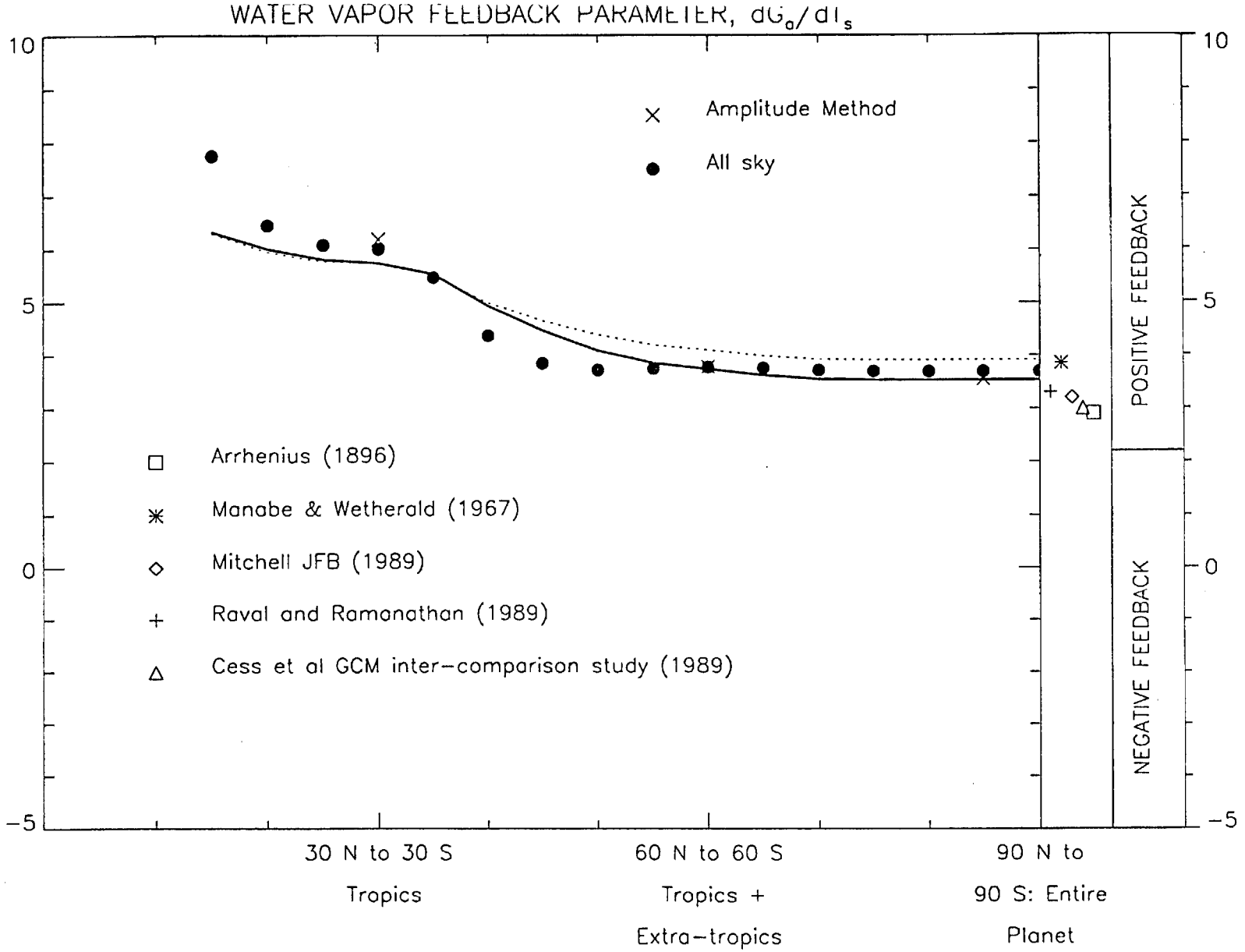

Fig. 5 Feedback sensitivity parameter, dG_a / dT_s, for different latitude ranges (Ocean + Land). The thick solid line depicts results which use the station data for the land surface temperatures (1988-89), while the dashed line employs the GEOS data. The results derived from the amplitude method (see text), and also the ERBE all-sky OLRs are shown by symbols. The equivalent estimates for the globe from other studies and GCM simulations are shown in the second right box, while the box at the extreme right marks the range of dG_a / dT_s into regions of positive and negative feedback.